Cell Reports, Volume *32*

Supplemental Information

A Non-Replicative Role of the 3′ Terminal Sequence of the Dengue Virus Genome in Membranous Replication Organelle Formation

Berati Cerikan, Sarah Goellner, Christopher John Neufeldt, Uta Haselmann, Klaas Mulder, Laurent Chatel-Chaix, Mirko Cortese, and Ralf Bartenschlager

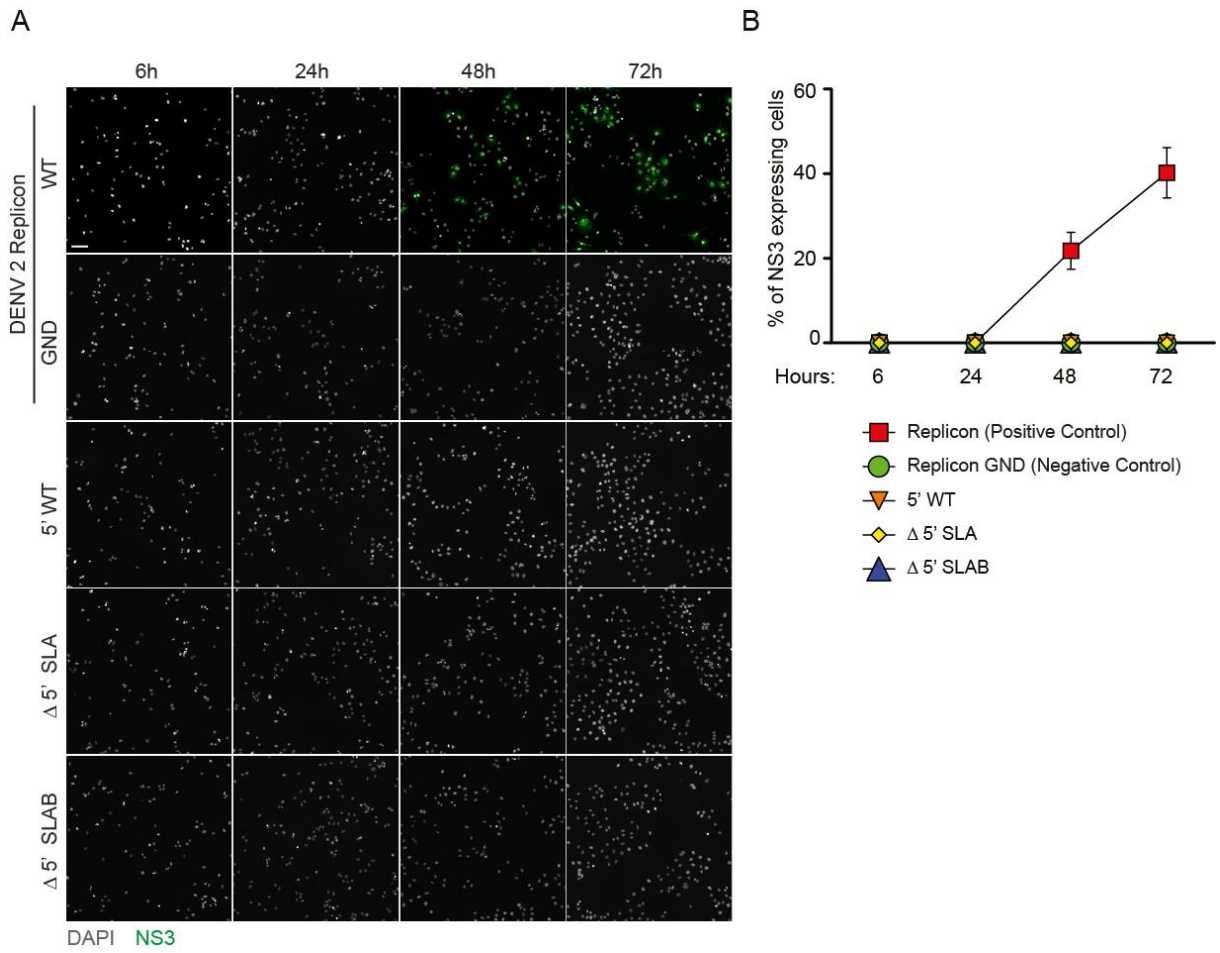

Figure S1. Related to Figure 2; in vitro transcripts derived from expression constructs 5' WT, Δ 5' SLA and Δ 5' SLAB are replication deficient.

(A) Representative immunofluorescence images used to determine replication competence of constructs specified on the left of each panel row. Subgenomic replicons sgDVR2A (wild type, WT) and sgDVR2A GND (replication deficient GND mutant) served as positive and negative controls, respectively. Scale bar: 100 µm. (B) Replication competence of each transcript was determined according to NS3-specific immunofluorescence staining and a custom made macro for the Fiji software package. Error bars represent the standard error of three independent experiments.

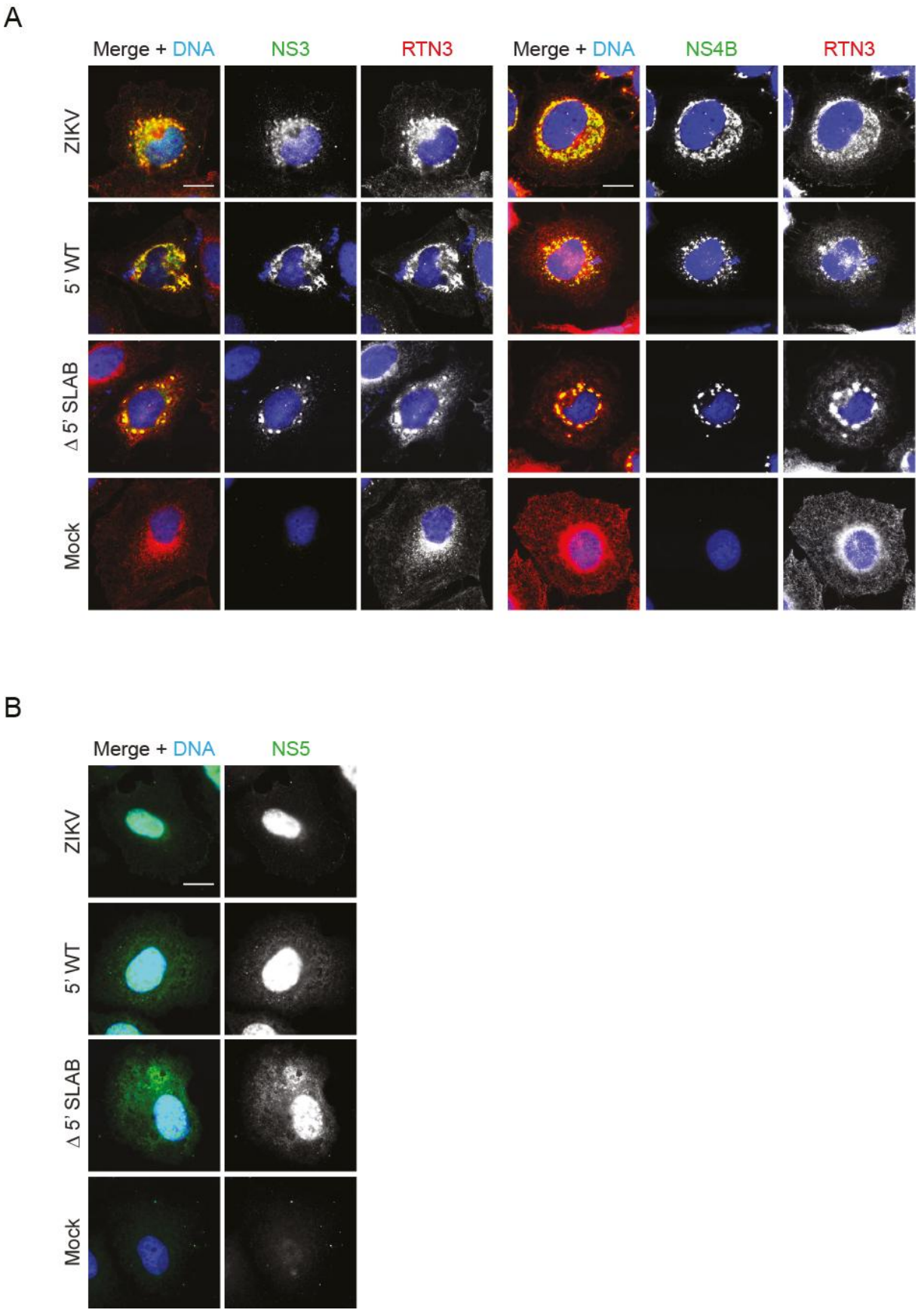

Figure S2. Related to Figure 3; Subcellular localization of ZIKV NS3, NS4B and NS5 in ZIKV 5' WT and Δ 5' SLAB transfected cells and ZIKV infected cells.

(A) Cells were either infected with ZIKV (upper row),or transfected with given constructs or left untreated (bottom row) and fixed for immunofluorescence analysis after 18 h in the case of transfections or 24 h after ZIKV infection (MOI=10). RTN3 (Reticulon 3) staining was used to visualize the ER. Scale bars: 10 μm. (B) Same as in A, but analyzing subcellular localization of ZIKV NS5. Scale bar: 10 μm.

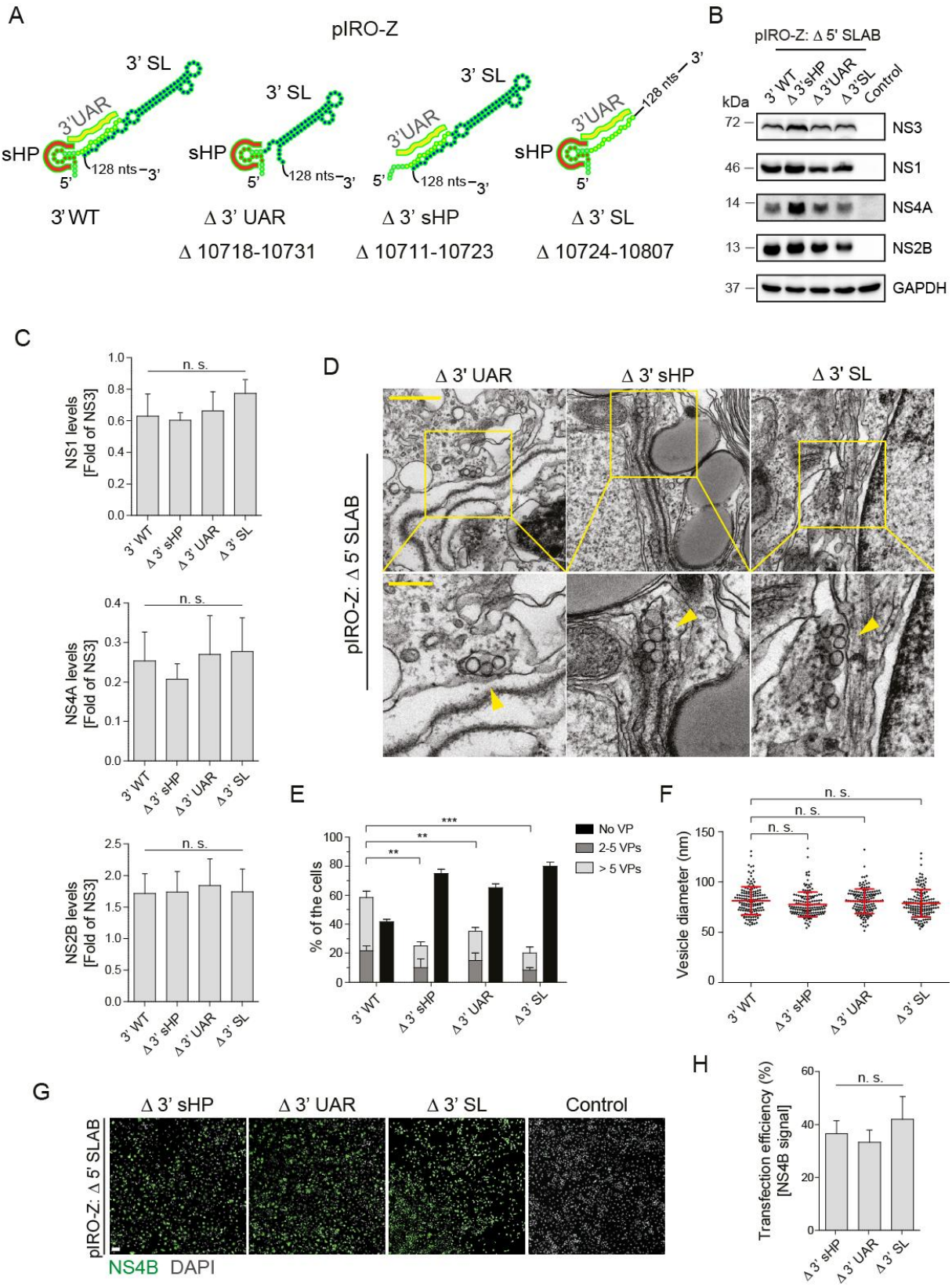

Figure S3. Related to Figure 6; Role of RNA elements in the 3' UTR of the ZIKV genome in replication organelle formation.

(A) Schematic representation of 3' UTR deletions introduced into the pIRO-Z Δ 5' SLAB construct. Numbers refer to the last nucleotide of the ZIKV genome contained in the expression construct (ZIKV H/PF/2013 strain;

GenBank accession number KJ776791.2). (B) Huh7/Lunet-T7 cells were either transfected with the parental construct containing the wild type (WT) 3' UTR (3' WT), or mock-transfected (Control) or transfected with indicated mutants. After 18 h cells were lysed and lysates analyzed by western blot. GAPDH served as sample loading control. (C) Relative ZIKV protein abundance was determined by densitometry of western blots and normalization of NS1, NS2B or NS4A values to those of NS3. Values represent mean and standard error of three independent experiments. n.s., not significant. (D) TEM images of Huh7/Lunet-T7 cells 18 h after transfection with indicated 3' UTR mutations introduced into the parental 3' WT construct. Fixed cells were processed and embedded into epon resin for sectioning. Lower panels are magnified views of areas indicated with yellow squares in the upper panel images. Yellow arrowheads indicate individual VPs. Scale bars: 500 nm and 200 nm (upper and lower panels, respectively). (E) For each condition, VPs contained in whole cell sections from 20 cells were counted. Means ± SEM from three independent quantifications are shown. ***, $p<0.001$; **, $p<0.01$. Quantification of 3' WT is taken from Figure 3F (construct Δ 5' SLAB). (F) Vesicle diameters were measured manually using the Fiji software package. Means ± SEM from three independent measurements (50 vesicles per experiment) are given. n.s., not significant. Vesicle diameter quantification of 3' WT is taken from Figure 3F (construct Δ 5' SLAB). (G) Detection of NS4B by immunofluorescence microscopy was used to determine transfection efficiency for the indicated constructs. The number of NS4B positive cells was normalized to total cell numbers. Scale bar: 100 μm. (H) Transfection efficiencies were quantified using NS4B. Error bars represent the standard error of three independent experiments. n.s., not significant.

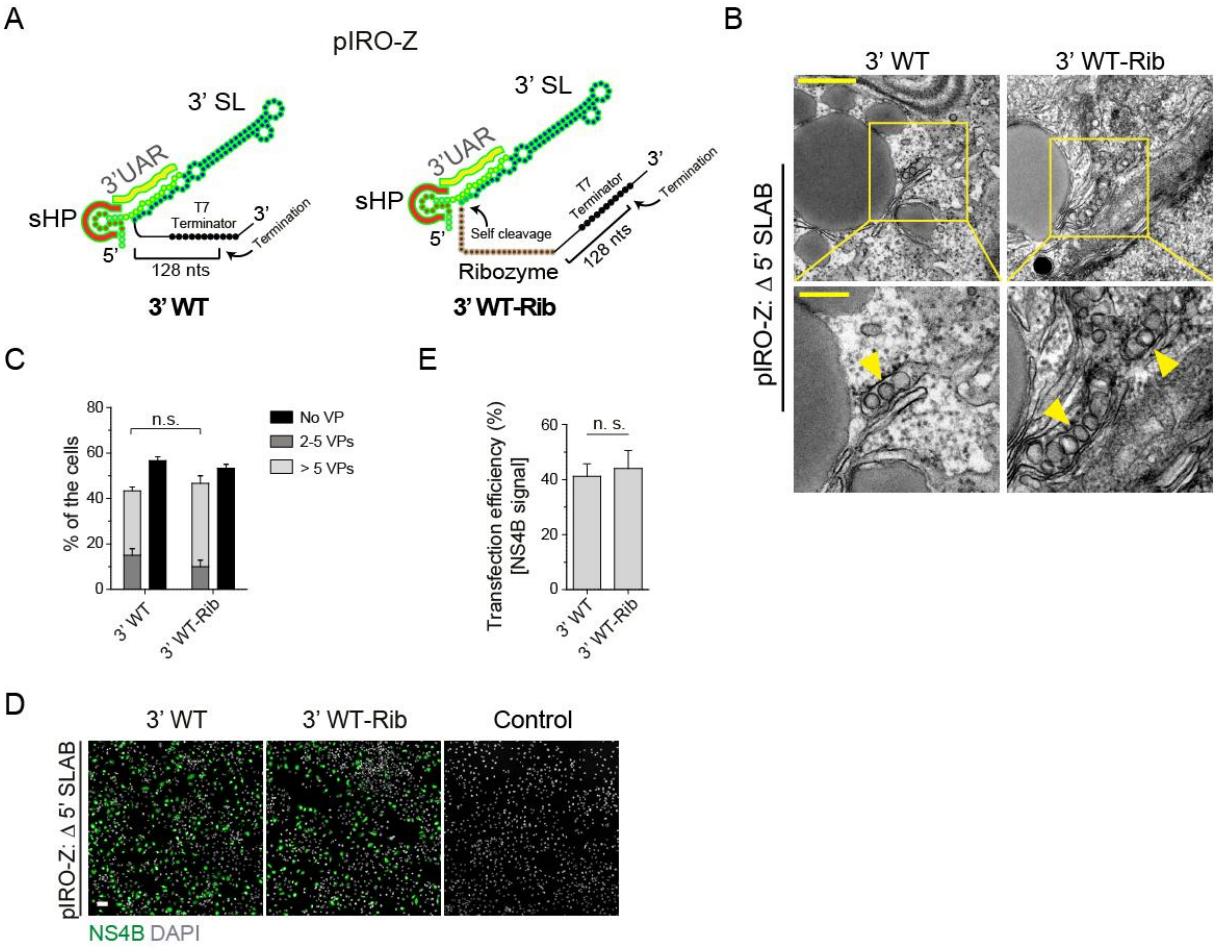

Figure S4. Related to Figure 7; No effect of the HDV ribozyme on ZIKV VP formation.

(A) Schematic representation of the 3' terminal regions of pIRO-Z Δ 5' SLAB constructs containing or lacking the HDV ribozyme. (B) TEM images of Huh7/Lunet-T7 cells transfected with the given pIRO-Z constructs. Cells were transfected and, 20 h later, fixed, processed and embedded in resin for sectioning. Lower panels are magnifications of yellow squared areas in the upper panel images. Yellow arrow heads indicate individual VPs. Scale bar in the upper and lower panel: 500 nm and 200 nm, respectively. (C) For each condition, VPs contained in whole cell sections from 20 cells were counted. Means ± SEM from three independent quantifications are given. n.s., not significant. (D) Detection of NS4B by immunofluorescence microscopy to determine transfection efficiency for the given constructs. Scale bar: 100 µm. (E) Transfection efficiencies were quantified by counting NS4B positive cells. Error bars represent the standard error of three independent experiments. n.s., not significant. Note that percentages given in (C) refer to all cells analyzed by TEM, but only ~40 % of them had been transfected (E) and therefore, not more than 40 % of cells can contain VPs.

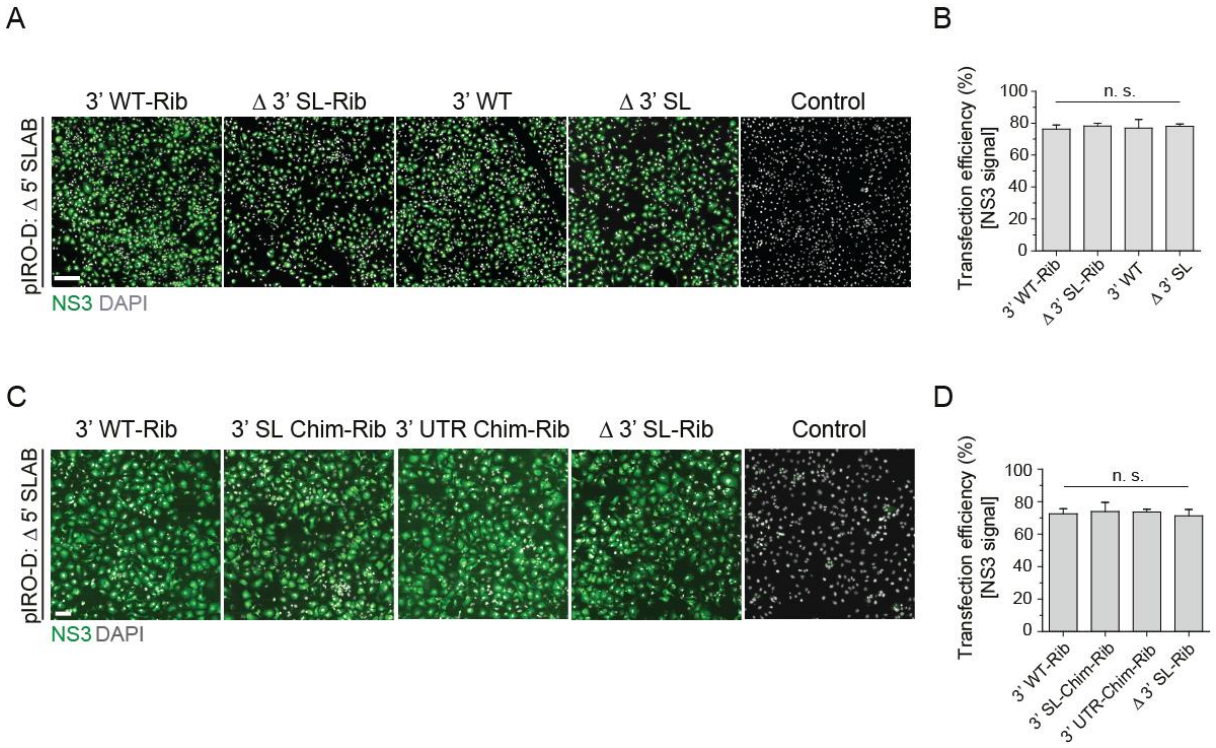

Figure S5. Related to Figure 7; Transfection efficiencies of pIRO-D HDV ribozyme containing constructs and chimeric constructs.

(A) Detection of NS3 by immunofluorescence microscopy to determine transfection efficiency for the given constructs. Scale bar: 500 µm. (B) Transfection efficiencies were quantified by counting NS3 positive cells and normalization to total cell number. Error bars represent the standard error of three independent experiments. n.s., not significant. Note that percentages given in (Figure 7C) refer to all cells analyzed by TEM, but only ~75 % of them had been transfected (B) and therefore, not more than 75 % of cells can contain VPs. (C, D) Transfection efficiencies achieved with constructs specified in each panel were determined using the same approach as described for panels A and B. Scale bar in (C): 100 µm. Error bars represent the standard error of three independent experiments. n.s., not significant.

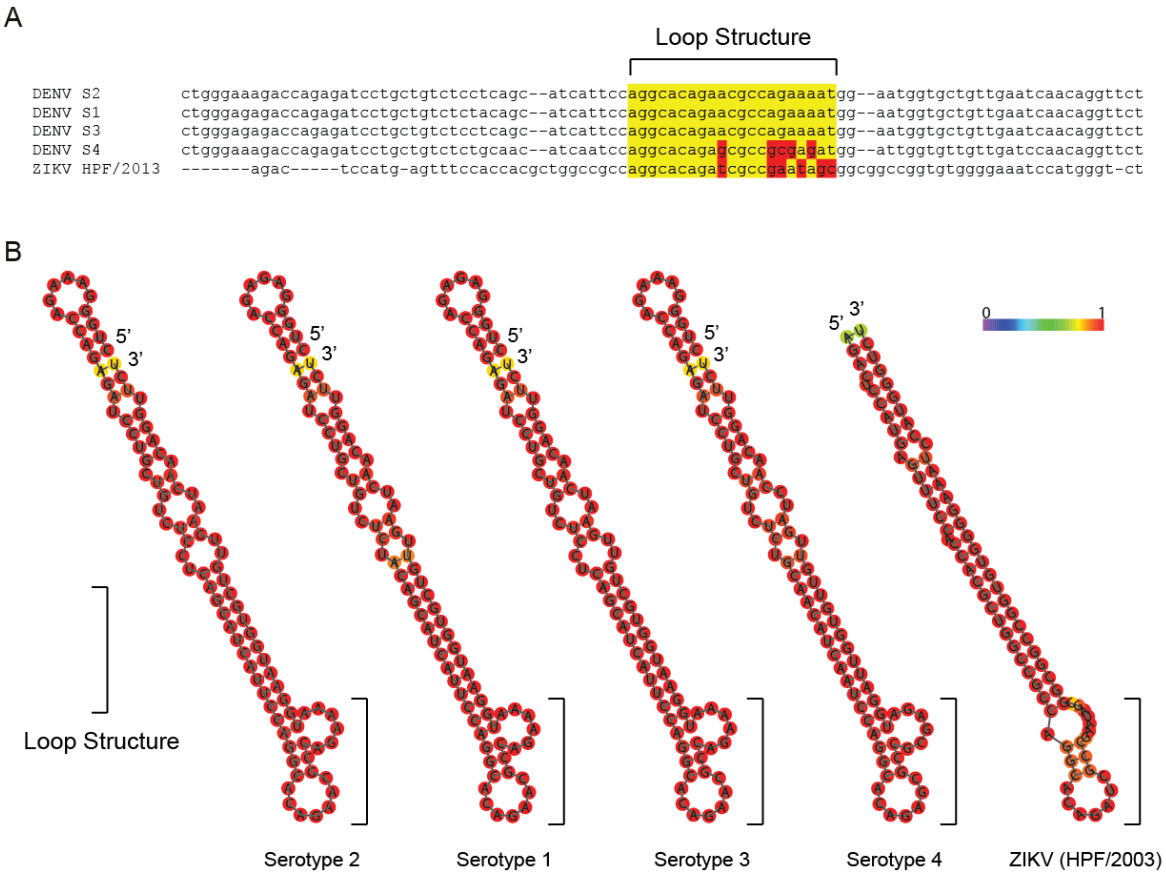

Figure S6. Related to Figure 7; Nucleotide sequence comparison and RNA secondary structure prediction of the 3' SL of DENV serotypes 1 - 4 and of ZIKV.

(A) Nucleotide sequence alignment of the 3' SL region of DENV serotypes 1, 3 and 4 and ZIKV (strain HPF/2013) with the 3' SL of DENV serotype 2. Sequence alignments were performed using the Clustal Omega program (EMBL-EBI). The RNA sequence corresponding to the loop structure is indicated with the yellow box. Nucleotide sequence differences are highlighted with red boxes. (B) Secondary structure predictions of the 3' SLs of the 4 DENV serotypes and of ZIKV (strain HPF/2013). Shown are minimal free energy drawings encoding base-pair probabilities. Color scale indicates base pairing probability with 0 being the lowest and 1 being the highest.

Table S1. Oligonucleotides for cloning. Related to Star methods-DNA plasmid constructs.

Primer sequences for DENV Δ 3' UAR mutant constructs
Fw: gcctggaatgatgctgaggctggtctttcccagcgtcaat
Rv: attgggttaacaagcagggccacctgggcaaa
Fw: attgacgctgggaaagaccagcctcagcatcattccaggc
Rv: tggtgagtactcaaccaagtcattctgagaatagtg
Primers sequences for DENV Δ 3' sHP mutant construct
Fw: ggagacagcaggatctctgcgtcaatatgctgttttttgtttc
Rv: attgggttaacaagcagggccacctgggcaaa
Fw: gaaacaaaaaacagcatattgacgcagagatcctgctgtctcc
Rv: tggtgagtactcaaccaagtcattctgagaatagtg
Primers sequences for DENV Δ 3' SL mutant construct
Fw: gatcgacttaataaggcttctagacagcaggatctctggtc
Rv: attgggttaacaagcagggccacctgggcaaa
Fw: gaccagagatcctgctgtctagaagccttattaagtcgatc
Rv: tggtgagtactcaaccaagtcattctgagaatagtg
Primer sequences for DENV 5' WT, Δ 5’ SLA, Δ 5’ SLAB mutant constructs
Fw_5' WT: gatcgacttaataaggcttctagacagcaggatctctggtc
Rv_ Δ 5’ SLA: attgggttaacaagcagggccacctgggcaaa
Fw_ Δ 5’ SLAB: gaccagagatcctgctgtctagaagccttattaagtcgatc
Rv: tggtgagtactcaaccaagtcattctgagaatagtg
Primer sequences for DENV 3' WT-Rib construct
Fw: ttgggttaacaagcagggccacctg
Rv: cggaatgttgcccagccggcgccagcgaggaggctgggaccatgccggccagaacctgttgattcaacagcaccattcc
Fw:gccggctgggcaacattccgaggggaccgtcccctcggtaatggcgaatgggacagaagccttattaagtcgatcgacgatccg
Rv: ggtgagtactcaaccaagtcattctgagaatagtgtatg
Primer sequences for DENV Δ 3' SL-Rib construct
Fw: ttgggttaacaagcagggccacctg
Rv: cggaatgttgcccagccggcgccagcgaggaggctgggaccatgccggccagacagcaggatctctggtctttcccag
Fw:gccggctgggcaacattccgaggggaccgtcccctcggtaatggcgaatgggacagaagccttattaagtcgatcgacgatccg
Rv: ggtgagtactcaaccaagtcattctgagaatagtgtatg
Primer sequences for DENV Δ 3' SL Chim-Rib construct
Fw: ttgggttaacaagcagggccacctg
Rv:cgccgctattcggcgatctgtgcctggcggccagcgtggtggaaactcatggagtctagacagcaggatctctggtctttcccag
Fw: cacagatcgccgaatagcggcggccggtgtggggaaatccatgggtctggccggcatggtcccagc
Rv: ggtgagtactcaaccaagtcattctgagaatagtgtatg

Primer sequences for DENV 3' UTR Chim-Rib construct
Fw: ttgggttaacaagcagggccacctg
Rv: ggtgagtactcaaccaagtcattctgagaatagtgtatg
Primer sequences for ZIKV 5' WT construct
Fw: gatcgcatgcccttattaagtcgatcgacg
Rv: gatcggcgcgccccctatagtgagtcgtattaatttc
Fw: gatcggcgcgccagttgttgatctgtgtgaatcagac
Rv: gatcgcatgcagacccatggatttccccac
Primer sequences for ZIKV Δ 5' SLAB mutant constructs
Fw: ataggggcgcgccatgaaaaacccaaaaaagaa
Rv: aagacccctaggaatgctcgtcaagaagaca
Primers sequences for ZIKV Δ 3' sHP mutant construct
Fw: aagttctagagatgcaagacttgtggc
Rv: atggagtctcgcgtcaatatgctgttttg
Fw: atattgacgcgagactccatgagtttccaccacg
Rv: gtggtgtcacgctcgtcgtttggtat
Primers sequences for ZIKV Δ 3' UAR mutant construct
Fw: aagttctagagatgcaagacttgtggc
Rv: aaactcatgtttcccagcgtcaatatgct
Fw: gctgggaaacatgagtttccaccacgctgg
Rv: gtggtgtcacgctcgtcgtttggtat
Primers sequences for ZIKV Δ 3' SL mutant construct
Fw: aagttctagagatgcaagacttgtggc
Rv: aaaagcatgcctggtctttccca
Primer sequences for ZIKV Δ 3' sHP-SL, Δ 3' CS-SL, Δ 3' complete mutant constructs
Fw: aagttctagagatgcaagacttgtggc
Rv_ Δ 3' sHP-SL: aaaagcatgccccagcgtcaatatgc
Rv_ Δ 3' CS-SL: aaaagcatgcgttttgcgttttccgg
Rv_ Δ 3' complete: aaaagcatgcttacagcactccaggtg